Proceedings of the 2015 International Conference on Machine Learning and Cybernetics, Guangzhou, 12-15 July, 2015

AN INTEGRATED FRAMEWORK FOR AERIAL IMAGE RESTORATION

NGAIMING KWOK[1] and HAIYAN SHI[2]

[1]School of Mechanical and Manufacturing Engineering, The University of New South Wales, Sydney, NSW, Australia
[2]School of Computer Science and Technology, Shaoxing University, Shaoxing, Zhejiang, China
E-MAIL: [1]nmkwok@unsw.edu.au, [2]csshy@usx.edu.cn

Abstract:

The restoration of aerial images is a crucial process for exposing ground features of interest to users. This is particularly important in applications concerned with the surveillance or remote sensing of the land. In this work, an efficient framework was developed that aims at providing a higher quality image of balanced tonal rendering, vivid colouring, and object boundary sharpening. These goals were achieved by processing the aerial image through an integration of colour channel mean value exponent alignment, pixel based min–max shifting and scaling, and object edge emphasizing. Real-world aerial images were used in experiments. Satisfactory results, evaluated both qualitatively and quantitatively, were obtained and verified the effectiveness of the proposed method.

Keywords:

Aerial image; Colour balance; Saturation enhancement; Contrast enhancement

1 Introduction

Vision based technology is a feasible and economic means for surveillance or monitoring of the environment. For example, it can be applied in road traffic regulation using cameras installed at elevated locations or aerial vehicles [1]. Such vision systems will be in great demand for managing emergency rescue and disaster relief [2].

Satellite images are also frequently used when a larger area or it is of interest in longer periods, such as during tropical cyclones, that have to be monitored [3]. However, hurdles that hinder their performances often arise from attenuation and scattering in optical transmission through the atmosphere [4]. Furthermore, occlusions from clouds may appear when a satellite image is captured [5], and shadows may cast on objects [6].

Other than using satellite images for surveillance purposes, aerial images captured from aeroplanes are also valuable sources of information. Unfortunately, these images still suffer from the same atmospheric degradation source as those satellite counterparts [7]. Problems including colour casting, reduced saturation, and loss of contrast have to be solved before a high quality aerial image can be made useful.

Here, an integrated framework is developed that aims to restore a degraded aerial image. The purpose is to balance the colour cast, increase the colour vividness, and to enhance the contrast. It contains stages involving the application of the grey-world assumption to align the mean values of the tristimuli channels for colour cast removal, then follows by a shift and scale operation on the minimum and maximum components of each pixel to improve colour saturation. Finally, the unsharp masking strategy is adapted to emphasis the object edges to improve the image contrast.

The rest of the paper is organized as follows. In Section 2, related work on aerial image restoration is briefly reviewed. The development of the proposed framework is detailed in Section 3. Section 4 describes the experiment and evaluates the results. A conclusion is drawn in Section 5.

2 Related Work

An aerial image is captured where objects are located on the ground while the camera is at an elevated altitude. The incident light onto the object, in most cases, is the sun light that passes through the atmosphere. Similarly, the reflected light also travels to the camera through the atmosphere [4].

Due to attenuation and scattering, in accordance with the light wavelength, the colour of the captured object may drift and has to be restored. In the work reported in [7], the colour tone discrepancy was eliminated by estimating the atmosphere characteristics from a reference image if available. Other approaches based on the grey world assumption [8][9][10] had produced satisfactory results. In essence, these methods align the mean values of each colour channel to a reference level,

978-1-4673-7220-6/15/$31.00 ©2015 IEEE

usually taken as the mean brightness value of the image. These two methods differ in the manner whether alignment is conducted linearly or exponentially, where the latter strategy is free of the over-range problem.

It is observed that because of scattering, sun light reaching particles in the atmosphere is deflected to the camera without reaching the object. This phenomenon results in a dilution of the saturation of the captured image. In order to improve the saturation, manipulations were made on the maximum pixel magnitude among tri-stimuli channels [11]. This method makes use of a retinex filter to separate the incident illumination and the reflected light from objects. However, the computation cost may be expensive. In addition, colours may be rendered into invalid regions and introduces the gamut problem [12].

Further to the enhancement of aerial image contrast, a number of approaches can be employed. The basic strategy involves globally processing the image in terms of relocating its brightness to a uniform or smoothed distribution [13]. In some cases, localized manipulation on the object edges is more effective to highlight the contrast around regions of interest. The unsharp masking filer is an attractive choice in this regard [14][15].

The above mentioned methodologies, although providing satisfactory results in specific problem domains, may not perform well when it is required to restore an aerial image that can satisfy a multiple of performance measures. An integrated framework is thus developed here addressing wider objectives including colour drift reduction, saturation increment and contrast enhancement.

3 Aerial Image Restoration Framework

The proposed aerial image restoration framework is depicted in Figure 1. It contains a collection of processes structured in a pipeline as shown. The cascaded stages include colour channel alignment to the global mean value for colour balancing, min–max pixel magnitude stretching for improved saturation, and an unsharp masking filter based contrast enhancement process. In particular, the procedures are efficient in the sense that no time consuming colour space transformation is needed.

3.1 Colour Balancing

Let the input aerial image $\mathcal{I}$ be given in the tri-stimuli, red (R), green (G), and blue (B) colour channels

$$\mathcal{I} = \{I(u,v)\} = \{R(u,v), G(u,v), B(u,v)\} \in [0,\ 1], \quad (1)$$

where (u, v) is the pixel coordinate and the magnitudes are normalized in the range $[0,\ 1]$. The coordinates may be dropped in the rest of the paper if it is clear from the context.

The grey-world assumption is invoked which states that the averaged image colour is grey thus removing the colour cast. This assumption holds if the mean values of the tri-stimuli channels are aligned. Based on the work reported in [8], the colour values are exponentially adjusted to satisfy this requirement. Furthermore, the use of exponent ensures that all manipulated pixel values are closed in the range $[0,\ 1]$. Here, the minimum of mean brightness of each input colour channel is first calculated, that is

$$I_\mu = \min_C \left\{ \frac{1}{N} \sum_{u,v} I^C \right\}, \quad (2)$$

where N is the total number of pixels, and the pixel colour magnitude is given by I^C for $C \in \{R, G, B\}$. For an image of size U-by-V (width by height), $N = U \times V$. The summation is carried out for the three colour components for all pixels.

Then the average values of each channel are determined as

$$I^C_\mu = \frac{1}{N} \sum_{u,v} I^C. \quad (3)$$

Each colour channel is further aligned to the image mean brightness by raising each pixel to an exponent. We have

$$I^C \leftarrow (I^C)^{\varphi^C},\ \varphi^C = \frac{\log(I_\mu)}{\log(I^C_\mu)} \quad (4)$$

where φ^C is the exponent for each individual colour.

3.2 Saturation Improvement

After removing the colour cast, the interim image is processed for saturation improvement. The method developed is motivated by examining the definition of colour saturation S in both the hue-saturation-intensity (HSI) and hue-saturation-value (HSV) colour spaces. From the definitions

$$S_{HSI} = 1 - \frac{3 \times \min\{R, G, B\}}{R + B + G} \quad (5)$$

$$S_{HSV} = 1 - \frac{\min\{R, G, B\}}{\max\{R, G, B\}}, \quad (6)$$

it can be seen that the saturation in both spaces can be increased if $\min\{R, G, B\}$ is compressed while $R + B + G$, or equivalently $\max\{R, G, B\}$, is amplified. The procedure for saturation improvement contains two stages. First, the pixel magnitudes are globally aligned to cover $[0,\ 1]$. That is

$$I^C \leftarrow \frac{I^C - \min_{C,uv}\{I\}}{\max_{C,uv}\{I\} - \min_{C,uv}\{I\}}, \quad (7)$$

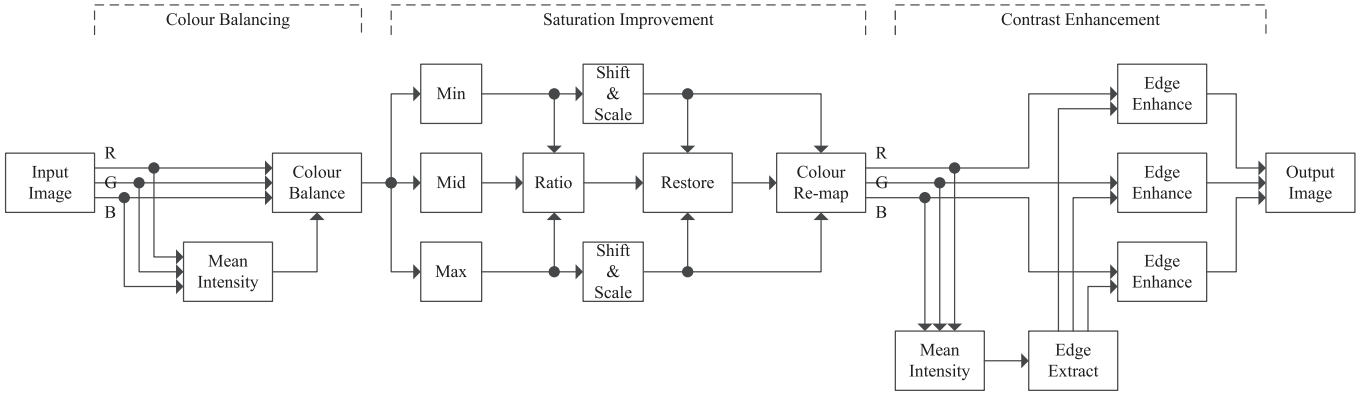

Figure 1: Aerial image enhancement framework

where the minimum and maximum are determined over all colour channels and all pixels. After this process, there is at least one pixel with the minimum colour at zero, and at least one pixel whose maximum colour is at unity. Thus, according to the definition of saturation, pixel saturations are partially improved.

The second stage involves sorting the colours of each pixel into the minimum (ε), middle (ς), and maximum (φ) elements such that $\varepsilon < \varsigma < \varphi$. Note that these three sets of elements are colour independent. Furthermore, a magnitude variable α defining the ratio of the middle element to the min–max range is calculated for post-normalization purpose. We have

$$\alpha = \frac{\varsigma - \varepsilon}{\varphi - \varepsilon}. \tag{8}$$

Then the minimum and maximum elements are compressed and expanded according to

$$\varepsilon \leftarrow (1-\gamma)\varepsilon,\ \varphi \leftarrow \gamma + (1-\gamma)\varphi,\ 0 < \gamma < 1. \tag{9}$$

This operation is, in fact, a shift-and-scale process depending on the parameter γ. It is worth to point out that the operation is magnitude closed where the resultant elements are kept in the range $[0,\ 1]$, thus, the gamut problem is avoided.

In order to reduce colour shift due to changes in the minimum and maximum element magnitude, the middle element is restored to its original ratio between the minimum and maximum elements. That is

$$\varsigma \leftarrow \alpha \times (\varphi - \varepsilon) + \varepsilon. \tag{10}$$

Finally, the elements are re-mapped to the corresponding colour channels according to their respective sorting index. At this stage, an image of improved saturation is obtained.

3.3 Contrast Enhancement

Following the improvement in image saturation, a contrast enhancement process focusing on the image brightness is carried out. The principle from unsharp masking filter [16] is employed in this stage.

First, then pixel-wise average values are calculated to represent the brightness. We have

$$B = \frac{1}{3}\sum_{C} I^C. \tag{11}$$

Then an 8-connected Laplacian kernel $\mathcal{K}$ is used to extract edges E from the brightness. That is

$$E = B \otimes \mathcal{K}, \tag{12}$$

where $\otimes$ is the convolution operator. Furthermore, the extracted edge is modulated by the brightness to avoid the over-enhancement problem. We have

$$E \leftarrow E \times (0.5 - |B - 0.5|). \tag{13}$$

Thus, when B is near the extreme ends of range $[0, 1]$, the corresponding modulated edges are reduced towards zero. On the other hand, when $B \approx 0.5$, the extracted edge magnitude approaches 0.5 and is the largest. The modulated edge is further scaled and superimposed onto the saturation improved image to produce a restored higher contrast output. That is

$$I^C \leftarrow I^C + \lambda E,\ \forall C \in \{R, G, B\}, \tag{14}$$

where λ is a control parameter determining the strength of enhancement. In addition, it also limits the amount of over-enhancement.

(a) (b) (c) (d)

Figure 2: Test image 1: (a) input, (b) colour balanced, (c) saturation improved, (d) contrast enhanced.

(a) (b) (c) (d)

Figure 3: Test image 2: (a) input, (b) colour balanced, (c) saturation improved, (d) contrast enhanced.

4 Experiments

Experiments were conducted to verify the effectiveness of the proposed aerial image restoration framework. Test aerial images were obtained from the USC-SIPI image database http://sipi.usc.edu/database/database.php?volume=aerials&image=36#top. These images were originally stored in the TIFF colour format. A total of 30 images, generated from cropping different regions on the downloaded images and resized to 480×640 pixels width-by-height, were used in the experiment. Parameters were set to $\gamma = 0.05$ (Eq. 9), and $\lambda = 0.35$ (Eq. 14) after some pilot experiments. Results were assessed both qualitatively and quantitatively according to several widely used criteria [17].

4.1 Qualitative Evaluation

Two sample test aerial images and their results are shown in Figures 2 and 3. It is observed that input images, Figures 2a and 3a, contain colour shifts due to colour selective absorption in the atmosphere. Furthermore, due to attenuation, saturation and contrast are both low. For those input images, users may find difficulties in identifying the objects captured.

Results from colour cast removal are given in Figures 2b and 3b. It is obvious that the bluish cast, due to transmission through nitrogen particles, has been removed and the true colours are recovered. The saturation improvement process produced images of better colour vividness and are illustrated in Figures 2c and 3c verifying the effectiveness of the process.

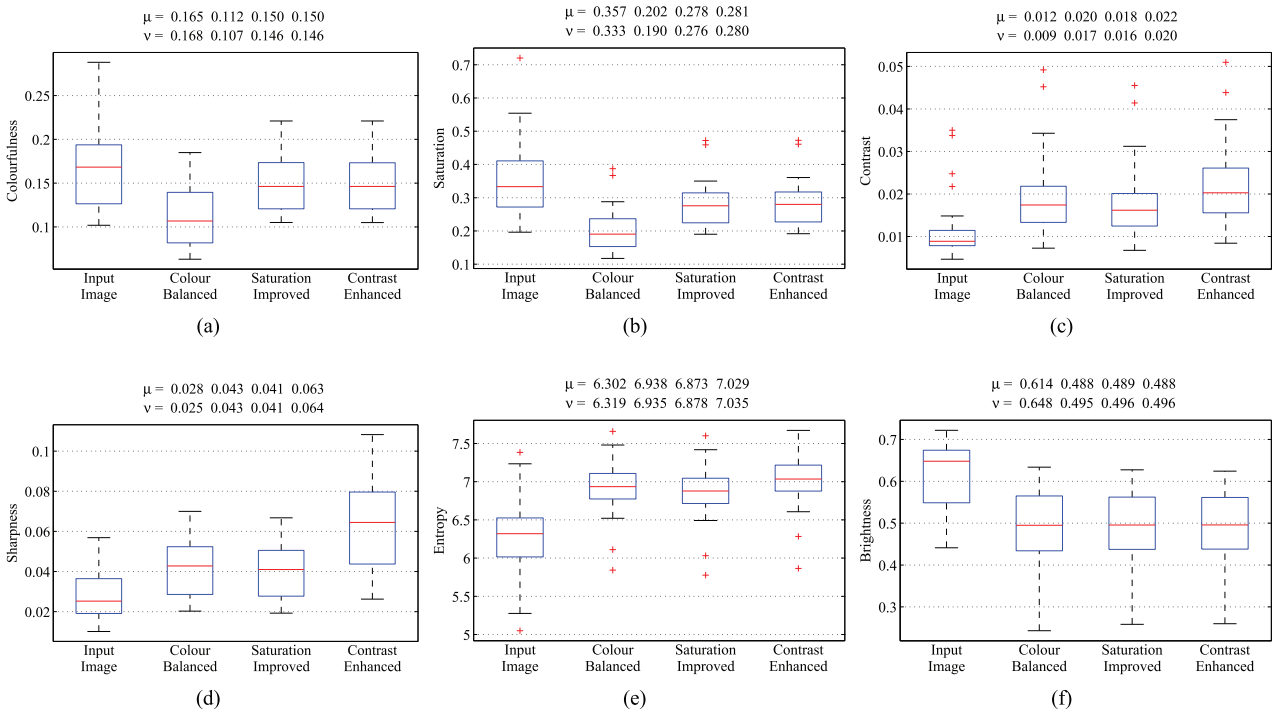

Figure 4: Results statistics; (a) colourfulness, (b) saturation, (c) contrast, (d) sharpness, (e) entropy, (f) brightness.

The final contrast enhancement stage outputs aerial images are shown in Figures 2d and 3d. Obviously, details of fine textures are being highlighted especially over the infrastructure and built areas on the ground. For aerial images, the enhancement on fine details is a very desirable feature.

4.2 Quantitative Evaluation

Statistics were collected from the 30 test image results against performance criteria including; colourfulness, average saturation, contrast, sharpness, entropy and average brightness. These metrics are depicted in box plots and shown in Figure 4. The mean (μ) and median (ν) values are included as annotations above the plots.

Results for colourfulness are shown in Figure 4a. Because the colour cast in the input image biases the colour tone, the colourfulness is higher than the processed results. On the other hand, a reduction or averaging out the colour tone indicates a desirable cast-free aerial image. Figure 4b shows the statistics concerning the average saturation. Since the input images are dominated by a relatively purer and saturated bluish tone, an improvement on the overall saturation is indicated by a lowering of averages resulted from the restoration stages.

Measures related to fine object details, include the contrast, sharpness and entropy are plotted in Figures 4c, 4d and 4e. Since these performance metrics are independent of colour tone, increases as compared to the input image, show that both local and global measures of contrast indicate that higher quality images are obtainable from the proposed restoration framework. The box plot of image brightness is given in Figure 4f. It is observed that the brightness is relocated to the mid-range of the permitted brightness magnitudes. This indicates that illumination bias due to atmospheric scattering has been removed and allows the resultant image for a better representation of the scene captured.

In summary, colour balancing has contributed to a significant mitigation of atmospheric caused colour tone casting. Subsequent processes for saturation improvement and contrast enhancement have further increase the aerial image quality.

5 Conclusion

An integrated framework was presented that aims at restoring atmospheric degraded aerial images with regard to the re-

moval of colour cast, improvements on image saturation and enhancements on contrast. Staged procedures were developed including aligning the mean values of each colour channel to the global pixel average for colour balancing. It was followed a compression on the minimum colour channel and an amplification on the maximum colour channel to improve image saturation. Then edge based emphases were superimposed to enhance the image contrast. Experimental results had shown that high quality aerials could be obtained so that subsequent user or computer based operations can be satisfactorily carried out.

References

[1] S. Zhang, W. Wang, S. Liu, and X. Zhang, "Image enhancement on fractional differential for road traffic and aerial images under bad weather and complicated situations," *Transportation Letters: the International Journal of Transportation Research*, vol. 6, no. 4, pp. 197–205, 2014.

[2] H. Ma, N. Lu, L. Ge, Q. Li, X. You, and X. Li, "Automatic road damage detection using high-resolution satellite images and road maps," in *Geoscience and Remote Sensing Symposium (IGARSS), 2013 IEEE International*. IEEE, 2013, pp. 3718–3721.

[3] K. Wang, X. Li, and L. Ge, "Locating tropical cyclones with integrated sar and optical satellite imagery." in *Geoscience and Remote Sensing Symposium (IGARSS), 2013 IEEE International*, 2013, pp. 1626–1629.

[4] H. Fallah-Adl, J. JáJá, S. Liang, J. Townshend, and Y. J. Kaufman, "Fast algorithms for removing atmospheric effects from satellite images," *Computational Science & Engineering, IEEE*, vol. 3, no. 2, pp. 66–77, 1996.

[5] M. Xu, X. Jia, and M. Pickering, "Automatic cloud removal for landsat 8 oli images using cirrus band," in *Geoscience and Remote Sensing Symposium (IGARSS), 2014 IEEE International*. IEEE, 2014, pp. 2511–2514.

[6] S. Wang and Y. Wang, "Shadow detection and compensation in high resolution satellite image based on retinex," in *Image and Graphics, 2009. ICIG'09. Fifth International Conference on*. IEEE, 2009, pp. 209–212.

[7] Y. Shen and S. K. Jakkula, "Aerial image enhancement based on estimation of atmospheric effects," in *Image Processing, 2007. ICIP 2007. IEEE International Conference on*, vol. 3. IEEE, 2007, pp. III–529.

[8] N. Kwok, D. Wang, X. Jia, S. Chen, G. Fang, and Q. Ha, "Gray world based color correction and intensity preservation for image enhancement," in *Image and Signal Processing (CISP), 2011 4th International Congress on*, vol. 2. IEEE, 2011, pp. 994–998.

[9] Y. Wang and Y. Luo, "Color constancy using bright-neutral pixels," *Journal of Electronic Imaging*, vol. 23, no. 2, pp. 023 011–023 011, 2014.

[10] N. Kwok, H. Shi, Q. P. Ha, G. Fang, S. Chen, and X. Jia, "Simultaneous image color correction and enhancement using particle swarm optimization," *Engineering Applications of Artificial Intelligence*, vol. 26, no. 10, pp. 2356–2371, 2013.

[11] W. Sun, L. Han, B. Guo, W. Jia, and M. Sun, "A fast color image enhancement algorithm based on max intensity channel," *Journal of Modern Optics*, vol. 61, no. 6, pp. 466–477, 2014.

[12] S. K. Naik and C. Murthy, "Hue-preserving color image enhancement without gamut problem," *Image Processing, IEEE Transactions on*, vol. 12, no. 12, pp. 1591–1598, 2003.

[13] N. M. Kwok, X. Jia, D. Wang, S. Chen, G. Fang, and Q. P. Ha, "Visual impact enhancement via image histogram smoothing and continuous intensity relocation," *Computers & Electrical Engineering*, vol. 37, no. 5, pp. 681–694, 2011.

[14] C. Yin, Y. Zhou, S. Agaian, and C. P. Chen, "Parametric rational unsharp masking for image enhancement," in *IS&T/SPIE Electronic Imaging*. International Society for Optics and Photonics, 2014, pp. 90 190W–90 190W.

[15] N. Kwok, H. Shi, G. Fang, and Q. Ha, "Adaptive scale adjustment design of unsharp masking filters for image contrast enhancement," in *Machine Learning and Cybernetics (ICMLC), 2013 International Conference on*, vol. 2. IEEE, 2013, pp. 884–889.

[16] N. Kwok and H. Shi, "Design of unsharp masking filter kernel and gain using particle swarm optimization," in *Image and Signal Processing (CISP), 2014 7th International Congress on*. IEEE, 2014, pp. 217–222.

[17] G. Jiang, C. Wong, S. Lin, M. Rahman, T. Ren, N. Kwok, H. Shi, Y.-H. Yu, and T. Wu, "Image contrast enhancement with brightness preservation using an optimal gamma correction and weighted sum approach," *Journal of Modern Optics*, vol. 62, no. 7, pp. 536–547, 2015.